Theoretical prediction on the coupling of thermoacoustic prime mover and RC load

Tang K., Chen GB., Jia Z.Z., Jiang N., Bao R.

Cryogenics Laboratory, Zhejiang University, Hangzhou 310027, China

The coupling of thermoacoustic prime mover and its load is of great importance for the performance of thermoacoustic system. A standing wave thermoacoustic prime mover with RC (resistance and capacitance) load is simulated, and the influence of RC load and dimensions of the resonance tube on the behavior of the thermoacoustic system is discussed according to the computed results.

INTRODUCTION

The ultimate purpose of the investigations on the thermoacoustic prime mover is to use it to drive a load, such as a pulse tube refrigerator or a thermoacoustic refrigerator etc. When the load is connected to the prime mover, the coupling between them is of great importance for the performance of the thermoacoustic system. In order to investigate the coupling relation, a standing wave thermoacoustic prime mover connected with an RC (resistance and capacitance) load is simulated with linear thermoacoustics [1]. The influence of some structure parameters (e.g. resistance and volume of RC load, length and inner diameter of resonance tube) on the performance of the system (e.g. frequency, acoustic power output, pressure amplitude, hot end temperature of stack) is discussed based on the computed results.

NUMERICAL SIMULATION

According to linear thermoacoustics [1], momentum, continuity and energy equations for a short channel dx can be written as:

$$\frac{dp_1}{dx} = -\frac{iwr_m}{1-f_n}\frac{U_1}{A} \tag{1}$$

$$\frac{dU_1}{dx} = -\frac{iwA}{gp_m}\left[1+(g-1)f_k\right]p_1 + \frac{f_k - f_n}{(1-f_n)(1-\mathrm{Pr})}\frac{1}{T_m}\frac{dT_m}{dx}U_1 \tag{2}$$

$$\frac{dT_m}{dx} = \frac{\dot{H}_2 - \frac{1}{2}\mathrm{Re}\left[p_1\tilde{U}_1\left(1-\frac{f_k-\tilde{f}_n}{(1+\mathrm{Pr})(1-\tilde{f}_n)}\right)\right]}{\frac{r_m c_p |U_1|^2}{2Aw(1-\mathrm{Pr}^2)|1-f_n|^2}\mathrm{Im}\left(f_k+\mathrm{Pr}\,\tilde{f}_n\right)-(Ak+A_{solid}k_{solid})} \tag{3}$$

where p_1 and U_1 are pressure and velocity amplitudes; w is angular frequency; r_m, T_m, c_p, g, k and Pr are mean density, temperature, isobaric specific heat, specific heat ratio, thermal conductivity and Prandtl number of working fluid, respectively; f_ν and f_κ are viscous and thermal functions; A is flow area of the channel; A_{solid} and k_{solid} are cross section area and thermal conductivity of the solid forming the channel;

$\dot{H}_2$ is total power; i is imaginary unit. Superscript ~ means the conjugation of a complex quantity.

The simulation for sanding wave thermoacoustic prime mover with an RC load, as shown in Figure 1, is carried out with Eqs (1)-(3). The main dimensions of the thermoacoustic prime mover and the RC are tabulated in Table 1. Working gas, heating power and working pressure are considered as He, 2000W and 2.0MPa, respectively, in the computation. Although R (resistance) of RC load is decided by the opening of the valve in practice, the value of R is directly given in the computation for simplifying the simulation. C (capacitance) of RC load can be calculated with $C = V / r_m a^2$, where V is the volume of the capacitance, r_m and a are mean density and acoustic velocity, respectively.

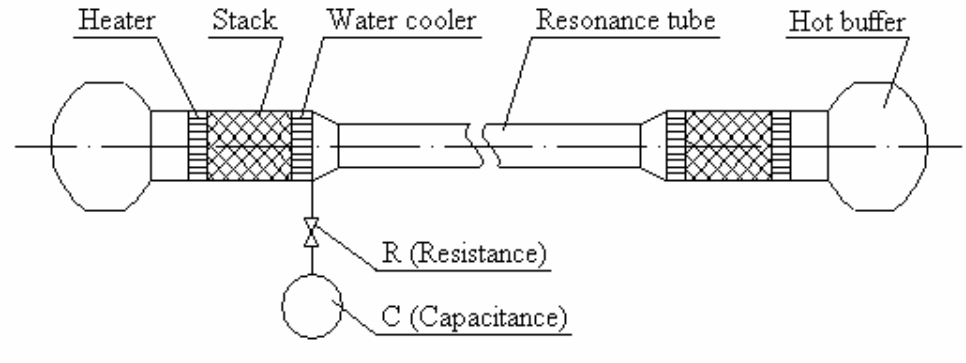

Figure 1 Schematic of thermoacoustic engine with RC load

Table 1 Dimensions of thermoacoustic engine and RC load

	Heater	Stack	Water cooler	Resonance tube	Hot buffer	Volume of C
Diameter (mm)	54	56	56	36-100 optional	/	/
Length (mm)	65	285	64	2000-10000 optional	(1.2L)	(0.25-1L optional)

COMPUTED RESULTS AND ANALYSIS

The influence of RC load on the performance of the thermoacoustic system is discussed with length and inner diameter of the resonance tube given as 4m and 36mm, respectively. Computed frequency with different volumes of C is shown in Figure 2. It can be seen that frequency increases slowly with accretion of R, and larger volume of C results in lower frequency, when R is smaller than 10^6 N.s/m^5. However, when R is in the range of 10^6 -10^8 N.s/m^5, frequency increases rapidly with accretion of R, and the increasing speed of larger volume of C is higher than that of smaller volume of C. When value of R is beyond 10^8 N.s/m^5, the increase of R leads to the decrease of frequency. Computed acoustic power output to RC load is presented in Figure 3. There is a peak along each of the curve with different volumes of C. Larger volume of C leads to a higher peak and a peak-shift in the direction of lower R. When R approaches to zero or infinity, the acoustic power output is almost zero. Figure 4 shows computed pressure amplitude at the inlet of RC load. In contrast with Figure 3, there is a valley along each of the curve with different volumes of C in Figure 4. Larger volume of C leads to a deeper valley and a valley-shift in the direction of lower R. The computed hot end temperature of the stack is presented in Figure 5. We can see that the forms of the curves in Figure 5 are similar to those in Figure 3.

Based on the comparison of all the forementioned figures, it is found that there is always a marked variation in the range of 10^6 -10^8 N.s/m^5 for R along all the curves. Further analysis indicates that the peaks in Figure 3 occur when R is almost equal to $1/wC$, that is, the equality of R and $1/wC$ results in maximum acoustic power output. These peaks lead to the valleys in Figure 4 and the peaks in Figure 5. It is because considerable part of the acoustic power generated by the stack is consumed by RC load in the

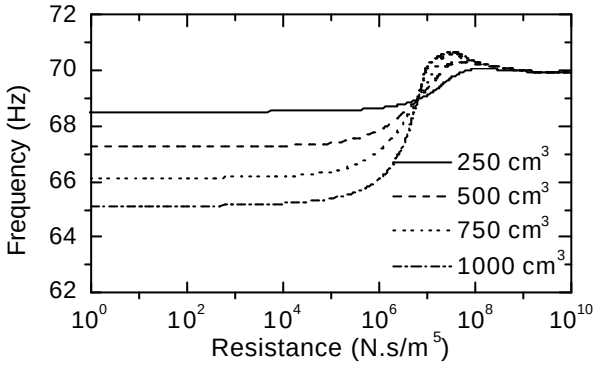

Figure 2 Computed frequency vs. R

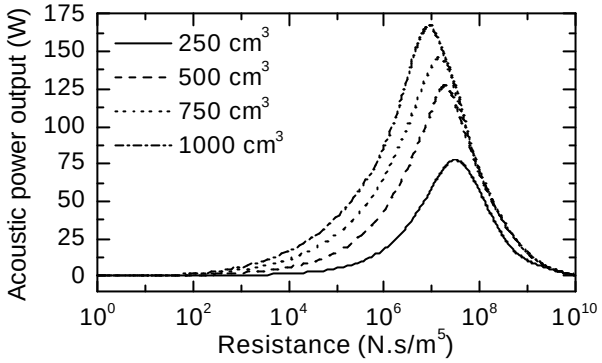

Figure 3 Computed acoustic power output vs. R

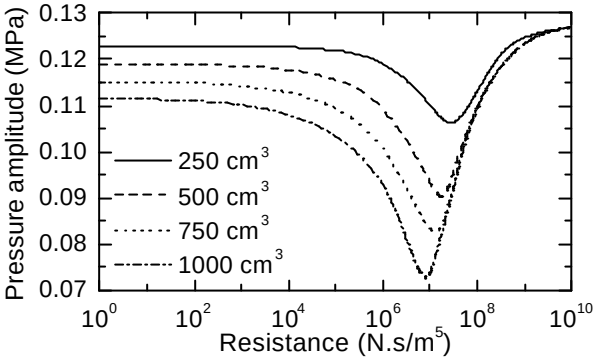

Figure 4 Computed pressure amplitude vs. R

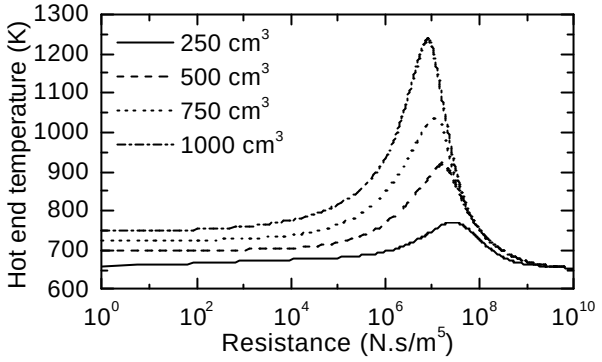

Figure 5 Computed hot end temperature of stack vs. R

peak region of Figure 3. This weakens the oscillating flow in the thermoacoustic system, and then, decreases the heat transfer in the stack, and induces an increase of stack's hot end temperature. Meanwhile, it is also found that the volume of C is a decisive factor for the performance of the thermoacoustic system when $1/wC$ is larger than R. In this case, an increase of volume of C may result in decreases of both frequency and pressure amplitude, as shown in Figure 2 and Figure 4, and may lead to increases of acoustic power output and stack's hot end temperature, as presented in Figure 3 and Figure 5. However, when R is larger than $1/wC$, the performance of thermoacoustic system is mainly dominated by R. Larger R induces lower frequency, less acoustic power output and lower hot end temperature of the stack, but higher pressure amplitude.

It is worthy of attention that the equalities of R and $1/wC$ are not always the best. Although acoustic power output is the maximum in this case, pressure amplitude is the minimum and hot end temperature of the stack is the highest. For a thermoacoustically driven pulse tube refrigerator, not only the input acoustic power but also the pressure amplitude is of great importance for the refrigeration performance. In addition, the hot end temperature of the stack can not be too high to the safety.

R and volume of RC load are fixed as 10^8 N.s/m^5 and 500 cm^3 for the computation of the resonance tube. Figure 6 presents the relation of frequency and L (length of the resonance tube) with different inner diameters. We can see that a longer and thinner resonance tube may realize a lower frequency. Computed pressure amplitude at the inlet of RC load is shown in Figure 7. It can be seen that the pressure amplitude increases with an accretion of resonance tube length initially, then decreases. The curves of computed acoustic power output to RC load, as shown in Figure 8, are similar to those of pressure amplitude in Figure 7. In order to explain the trend of the curves in Figure7 and Figure 8, acoustic power losses of components are computed with 56mm inner diameter resonance tube as an example and presented in Figure 9. Figure 9 indicates that the acoustic power loss of thermoacoustic core (composed of stack, heater and water cooler) is much high than that of any other component and dominates the behavior of thermoacoustic system when the resonance tube is short. In this case, a decrease of the acoustic power loss of thermoacoustic core with an increase of the resonance tube length enhances the oscillation and increases both the pressure amplitude and the acoustic power output. However, the acoustic power loss of resonance tube increases and catches up to that of the thermoacoustic core when the resonance tube is

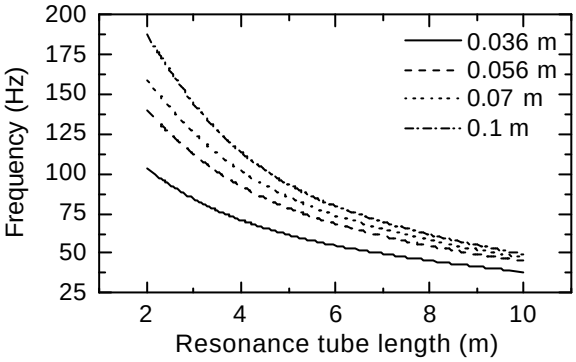

Figure 6 Computed frequency vs. L

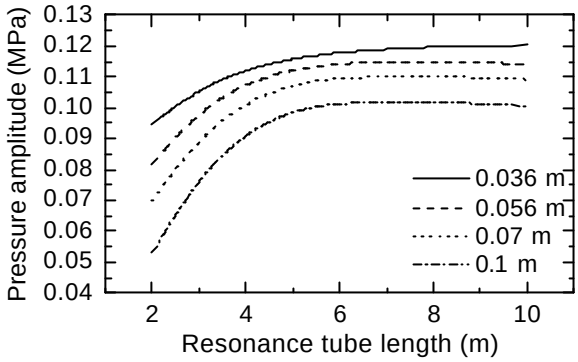

Figure 7 Computed pressure amplitude vs. L

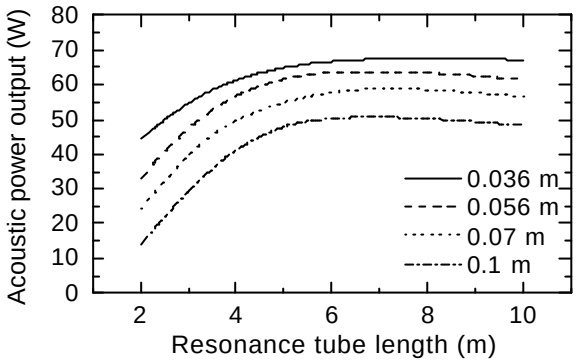

Figure 8 Computed acoustic power output vs. L

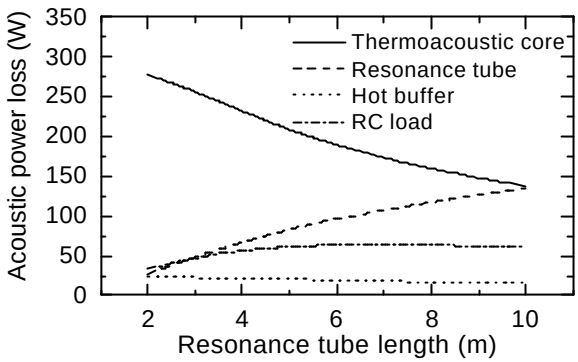

Figure 9 Computed acoustic power loss vs. L

prolonged further. Both the pressure amplitude and the acoustic power output decrease with an increase of resonance tube length when the acoustic power loss of the resonance tube is comparable or even beyond that of the thermoacoustic core.

CONCLUSIONS

The computed results indicate that the behavior of the thermoacoustic system is greatly influenced by the impedance of the load and the dimensions of the resonance tube. C of RC load is a key influencing factor when $1/wC$ is larger than R, while R is of great importance, when $1/wC$ is less than R. The maximum acoustic power output can be achieved when $1/wC$ equals to R, while pressure amplitude is the minimum and hot end temperature of the stack is the highest. Besides, there is an optimal value of resonance tube length for the maximum acoustic power output. A thinner resonance tube may lead to lower frequency, higher pressure amplitude and larger acoustic power output in the computation range.

ACKNOWLEDGMENT

The authors hope to express their appreciation for the National Natural Sciences Foundation of China (50376055) and the University Doctoral Subject Special Foundation of China (20010335010).

REFERENCES

1. Swift, G.W., Thermoacoustic engine, J.Acoust.Soc.Am. (1988) 84 1145-1180